Analysis of Sub-synchronous Oscillations in West Murray Zone Power System in Australia

July 2025

AEMO
AUSTRALIAN ENERGY MARKET OPERATOR

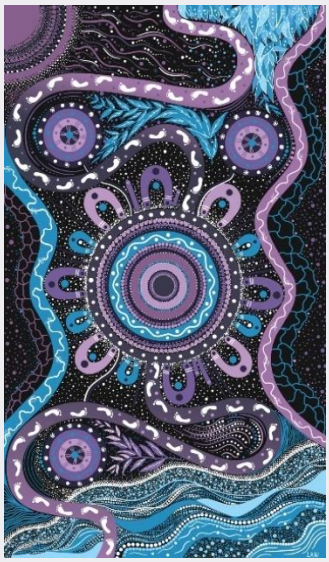

We acknowledge the Traditional Custodians of the land, seas and waters across Australia. We honour the wisdom of Aboriginal and Torres Strait Islander Elders past and present and embrace future generations.

We acknowledge that, wherever we work, we do so on Aboriginal and Torres Strait Islander lands. We pay respect to the world's oldest continuing culture and First Nations peoples' deep and continuing connection to Country; and hope that our work can benefit both people and Country.

'Journey of unity: AEMO's Reconciliation Path' by Lani Balzan

AEMO Group is proud to have launched its first Reconciliation Action Plan in May 2024. 'Journey of unity: AEMO's Reconciliation Path' was created by Wiradjuri artist Lani Balzan to visually narrate our ongoing journey towards reconciliation - a collaborative endeavour that honours First Nations cultures, fosters mutual understanding, and paves the way for a brighter, more inclusive future.

Important notice

Purpose

The purpose of this technical note is to provide detailed information about the power system oscillations that have been observed in the West Murray Zone power system in Australia. This technical note incorporates field observations, high-resolution measurement data and AEMO's approach to investigate root cause of the power system oscillations.

Impedance-based stability analysis framework are utilised in this report to uncover the root cause of the observed oscillations. The findings from the impedance-based stability analysis are corroborated using electromagnetic simulations and compared with the field-measurement data confirming the accuracy of AEMO's power system models. This work forms part of AEMO's Engineering Roadmap efforts to improve understanding of emerging power system stability phenomena using novel analytical tools.

Disclaimer

This document or the information in it may be subsequently updated or amended. This document does not constitute legal or business advice, and should not be relied on as a substitute for obtaining detailed advice about the National Electricity Law, the National Electricity Rules, or any other applicable laws, procedures or policies. AEMO has made reasonable efforts to ensure the quality of the information in this document but cannot guarantee its accuracy or completeness.

Accordingly, to the maximum extent permitted by law, AEMO and its officers, employees and consultants involved in the preparation of this document:

- make no representation or warranty, express or implied, as to the currency, accuracy, reliability or completeness of the information in this document; and
- are not liable (whether by reason of negligence or otherwise) for any statements or representations in this document, or any omissions from it, or for any use or reliance on the information in it.

Copyright

Executive summary

Voltage and power oscillations are a naturally occurring phenomena in electric power systems all over the world. If not planned for and managed they have the potential to disrupt power systems if they do not subside following a disturbance, such as a fault or a sudden loss of generation or load. Power systems are therefore designed to automatically subdue these oscillations, a process referred to as damping. If an oscillation is undamped, due to unusual operating conditions, poor design or faulty equipment, it will grow with a likely result being protection systems activating, leading to disconnection of loads, generation or even large sections of the power system.

AEMO and other system operators across the world have observed an increase in oscillation events. These events often manifest themselves under conditions where system strength is decreased, such as a transmission line outage or periods of high solar and low synchronous generation.

By utilising impedance scan techniques, it is now feasible to screen for sub-synchronous oscillations during the connection and operation of new IBRs. This allows for the adjustment of control systems to prevent potential oscillations from occurring during system operation.

Power systems with many synchronous generators have high inertia characteristics due to the kinetic energy stored in the rotating masses of the generator and turbine. This inertia helps provide a stable frequency and but can also result in low frequency (less than 0.5 Hz) oscillations between different regions of the grid, also known as inter-area oscillations. The damping of inter-area oscillations has been kept at acceptable levels through the coordinated tuning of power system stabilisers (PSS) on a relatively small number of large synchronous generators. However, retirement of synchronous generators equipped with PSS are expected to reduce the number of PSS devices available to contribute to damping.

Inverter-based resources (IBRs) are being deployed at a capacity many times (approximately 4:1) that of retiring synchronous generators to account for the intermittent nature of renewable energy. This volume of inverter-based resources presents further challenges in the form of sub synchronous oscillations (5-40 Hz) typically related to control system interactions between inverter-based resources. The control systems on these IBRs therefore need to be carefully managed and planned for to mitigate the potential for sub synchronous oscillations (SSOs) and increased risks to power system security through model simulation techniques and field measurements.

The emergence of increased oscillations in grids with high levels of IBR underscores the importance of both continued monitoring of power system oscillations with sufficient resolution at various locations in the grid, and the sustained development and deployment of appropriate solutions to manage them. Adequate monitoring systems together with appropriate analysis tools can help to improve understanding of power system oscillations, allowing efficient management.

Through the Engineering Roadmap, AEMO is proactively focusing on investigating emerging power system stability phenomena using novel analytical tools and identifying and developing appropriate remediation measures for complex stability problems.

In Australia, sub-synchronous oscillations have been observed in areas that have a large concentrations of IBRs. The frequency of oscillations has been between 7 hertz (Hz) and 10 Hz, and 17 Hz and 20 Hz, with varying magnitudes and durations. When a large part of the network is experiencing oscillations, it is important to understand the root cause. Identifying the root cause not only allows the system operator to eliminate the source of oscillations operationally, but also

provides an opportunity to work with relevant generation, storage and inverter-based load owners to explore long-term solutions.

Field measurements capturing oscillations at various nodes in the system can provide insights on the possible source of oscillations, or identify the region where the source of the oscillations is located. However, using only field measurements it is often difficult to answer more specific questions, such as whether any specific IBR or a group of IBRs are responsible for the oscillations. Such a measurement-based approach depends on the availability and quality of measurement data, and post-event analysis cannot provide any forecast nor any insight on the impact of various potential contributing factors on existing or future oscillation events.

Currently SSOs are identified through time domain electromagnetic transient (EMT) model simulation tools (PSCAD™), however, this analysis is time-consuming, computationally intensive and issues can be overlooked. Moreover, time-domain simulations do not always reveal the root cause of the oscillations without extensive sensitivity analysis being undertaken. The advancement of impedance-based frequency scan tools allows for scans of IBRs and the network at their points of connection and could provide useful and detailed insights to manage SSOs which were previously difficult to achieve through time domain EMT analysis.

This report presents an impedance scan analysis of intermittent power system sub-synchronous oscillations that have been observed by AEMO. Through the impedance scan of each of the IBRs, both individually and collectively, potential resonance modes have been identified. The impedance scans were carried out using electromagnetic transient (EMT) simulation models of the network. The network comprises site-specific, black-boxed models of IBRs supplied by the generators.

The impedance scan approach was divided into three major steps:

- Identification of IBRs where impedance analysis needed to be performed based on the magnitude of oscillations observed at their connection points.
- Undertaking impedance scans at selected IBRs in a single-machine infinite-bus (SMIB) configuration to identify internal resonance modes of the selected IBRs and to evaluate if any of these modes may became unstable under certain grid conditions.
- Undertaking impedance scans at IBRs while they were connected to the wider network model to obtain the impedance response of both the IBR and the grid to evaluate control interactions among IBRs.

The impedance scan analysis produced the following outcomes.

- A few IBRs have a resonance mode around 17 Hz, which becomes poorly damped or unstable under a certain operating condition.
- Two IBRs in the network under investigation forms a mode at 23 Hz when they operate at low irradiance condition. The mode has sufficient positive damping; however, the connection of another IBR during low irradiance condition pushes the 23 Hz mode to 17 Hz resonance frequency, and also reduces the damping to a negative value, creating sustained 17 Hz oscillations in the system.
- Certain IBRs increase the effective grid impedance seen by another IBR in close proximity for a particular operating condition. Under this operating condition, the resulting sub-synchronous oscillation mode is more pronounced due to a combination of control interactions among IBRs through the transmission network under study and a resonance mode inside the IBRs.

- The impedance analysis of the wide area network confirmed that certain IBRs alter the effective grid impedance at non-fundamental frequencies at the connection points of other IBRs. This finding highlights the limitations of metrics like Short Circuit Ratio (SCR), which only consider the fundamental frequency when assessing grid system strength. In contrast, impedance scans cover a broad frequency range and account for interactions with other IBRs.

The impedance scan analysis has demonstrated advantages over an iterative time-domain analysis approach using EMT models to identify potential instability issues resulting from sub-synchronous oscillations. The analysis provides confidence that future sub-synchronous oscillations may be investigated and addressed through a similar approach early in the connection process. AEMO has an ongoing program of works to further explore the use of such techniques during generator connection, system planning and system operation. AEMO is also actively collaborating with other system operators to understand their experience of using similar approaches in examining control interactions in IBR dominated power system.

Contents

Tables

Figures

1 Background

The Australian National Electricity Market (NEM) power system has been going through a significant transition in the past few years, from a centralised, fossil-fuel based power system, towards a power system with high penetration of inverter-based resources (IBRs). In Q4 2024, peak instantaneous renewable energy contributions reached 75.6% for the NEM power system. At this time, the potential NEM-wide renewable energy contribution reached 105.7%, with the difference between potential and dispatched contributions being primarily due to economic offloading. Renewable energy-driven IBRs such as distributed photovoltaics (PV), grid-scale solar farms, and wind farms contributed heavily to the maximum instantaneous renewable energy contribution and renewable potential, highlighting significant growth potential for future IBR contribution.

Figure 1 West Murray Zone (WMZ) – (a) Map of the WMZ, (b) RMS voltages at certain critical buses in the WMZ during a 17 Hz oscillation incident

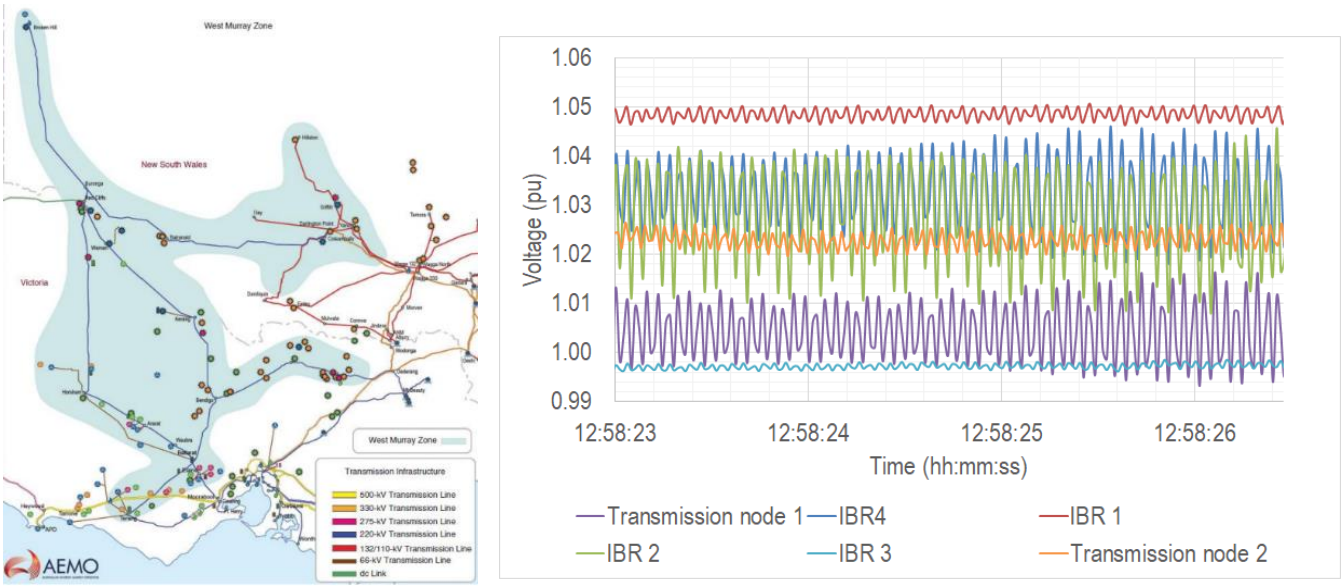

(a) (b)

Many IBRs in the NEM power system are connected in regions with relatively low system strength levels. The West Murray Zone (WMZ) is one such region, located in the north-west of Victoria, far away from synchronous generators and with abundant solar and wind resources. A map of the WMZ is shown in **Figure 1(a)**.

Between 2018 and 2023, AEMO observed two IBR-driven sub-synchronous oscillation (SSO) incidents in the WMZ region. The first incident in 2018 involved an 8 Hz voltage oscillation mode caused by five solar farms in this area; it was triggered by the disconnection of a nearby 220 kilovolts (kV) transmission circuit. AEMO identified the source of the 8 Hz oscillations via electromagnetic transient (EMT) time-domain simulations[1], and further eliminated the oscillations through controller

[1] B. Badrzadeh, N. Modi, N. Crooks, and A. Jalali, "Power system operation with reduced system strength for inverter-connected generation during prior outage conditions." CIGRE Science and Engineering Journal 17 (2020): 141-149.

retuning by working directly with the inverter original equipment manufacturer (OEM)[2]. Another SSO incident was observed in 2020 with voltage oscillations at a frequency of 17 Hz[3]. **Figure 1(b)** shows recorded root mean square (RMS) voltage at several critical buses in the WMZ during one occurrence of the 17 Hz oscillations.

The magnitude of the 17 Hz oscillations has remained relatively low with the highest level ever observed being 2.2% peak-to-peak on the 220 kV Red Cliff Terminal Station (RCTS).

Initial analysis conducted by AEMO using high-resolution measurements at several substations showed that the oscillations are contained in the area west of Bendigo and Darlington Point. Moreover, certain oscillation events occurred during the outage of the 220 kV Red Cliffs to Buronga transmission line and when the Murray Link (MLDC) was out of operation. This indicated that the source of oscillations lies within the north-west Victoria region.

While many of the 17 Hz oscillation events have occurred following a disturbance, some oscillation events happened spuriously in the absence of an obvious network disturbance. This further indicates that the operating condition of IBRs might be playing a critical role in the development of oscillations in addition to the system topology. It is critical to understand the root cause of these oscillations and mitigate the risk of potential threat to power system security, particularly because the increasing wind and solar generation and decreasing grid strength can further exacerbate the problem.

This report summarises the methodology and tools, study scenarios, analysis results, findings and recommendations from a work that AEMO and the National Renewable Energy Laboratory (NREL) jointly conducted to identify the root cause of 17 Hz SSO incidents observed in the WMZ power system, using the impedance-based stability analysis. The work leverages NREL's Grid Impedance Scan Tool (GIST) to evaluate the role of different inverter-based resources (IBRs) in the 17 Hz SSO events. This is achieved by performing impedance scans of selected IBRs as well as of the grid as seen from the IBR connection points from a EMT model of the WMZ power system.

[2] A. Jalali, B. Badrzadeh, J. Lu, N. Modi, and M. Gordon (2021), "System strength challenges and solutions developed for a remote area of Australian power system with high penetration of inverter-based resources," CIGRE Science and Engineering Journal, 27-37.

[3] AEMO, West Murray Zone Sub-synchronous oscillation, October 2022, at https://aemo.com.au/-/media/files/electricity/nem/network_connections/west-murray/high-level-summary-of-wmz-subsynchronous-oscillations.pdf?la=en.

2 Methodology and procedure

2.1 Study methodology

This section provides a simplified description of the impedance-based stability analysis methodology used for the analysis of the WMZ 17 Hz SSO incident. The impedance-based stability analysis relies on obtaining the frequency-domain impedance response of an IBR and the grid to which the IBR connects, and determine the stability of the IBR-grid system with the generalized Nyquist Criterion. This method can also be adopted for multi-IBR power systems. The methodology used in this project adopts theorems and procedures developed in many existing publications and applications from many researchers and industry entities[4,5]. This work seeks to apply these existing theorems to analyse the WMZ 17 Hz SSO incident, rather than varying them or developing any new theorem. Detailed description of these theorems and practices can be found in Appendix A1 of this report.

A two-part study methodology has been adopted for this work:

- Step 1, SMIB IBR Scan: The impedance response of a selected IBR, $Z_i(s)$, is obtained by connecting it to an infinite bus in single machine infinite bus (SMIB) configuration. The scanned impedance response is used to evaluate whether the IBR has any internal resonance modes with low damping and if the IBR becomes unstable when connected to an inductive grid with a particular short circuit ratio (SCR) and X/R ratio. The analysis is performed at a few operating points that cover the typical operational envelope of the IBR. Because the grid in this case, an infinite bus, is stable without the IBR, this step uses a standard approach[6] for the impedance-based stability analysis to identify grid condition in terms of SCR and X/R ratio under which the IBR might become unstable.
- Step 2, Wide Area Network Scan: The impedance response of the grid at the connection point of the selected IBR, $Z_g(s)$, is obtained using the wide area network EMT model including other IBRs. The grid impedance response is obtained for different operating and dispatch conditions of IBRs in proximity. The selection of scan conditions is done iteratively to evaluate how they influence control interactions among IBRs. The grid impedance scan is obtained using the integrated EMT model of the system with all the IBRs connected to the grid. This integrated EMT model of the system must be stable to perform the grid impedance scan. Hence, a reversed approach[7] of the impedance analysis is used first to determine if the grid will remain stable if the IBR to be scanned is removed. If the analysis using the reversed criterion shows that the grid becomes unstable without the IBR, it shows this IBR is contributing positive damping to the system and it is critical for the grid stability. On the other hand, if the analysis shows that the grid will remain stable without the IBR, the impedance analysis is performed using the scanned grid impedance, $Z_g(s)$, in conjunction with the IBR impedance scans, $Z_i(s)$, obtained in the first step of SMIB IBR scans. This second part of the analysis using the Wide Area Network Scan uses both the standard and reversed approaches for the stability analysis.

[4] M. Cespedes and J. Sun, "Impedance Modeling and Analysis of Grid-Connected Voltage-Source Converters," in IEEE Transactions on Power Electronics, vol. 29, no. 3, pp. 1254-1261, March 2014

[5] S. Shah, P. Koralewicz, V. Gevorgian, H. Liu, and J. Fu, "Impedance methods for analyzing stability impacts of inverter-based resources: stability analysis tools for modern power systems," IEEE Electrification Magazine, vol. 9, no. 1, pp. 53-65, Mar. 2021

[6] Refer to Appendix A1.1 for detailed description of this approach.

[7] Refer to Appendix A1.3 for detailed description of this approach.

The above steps are performed successively at different IBRs of interest to evaluate how each of them impact the frequency and damping of the oscillation modes in the WMZ in the frequency range where oscillations have been observed in the field.

2.2 Study procedure

Based on field measurements of the voltage oscillation data recorded by PMUs in the WMZ, the oscillation likely involved some IBRs connected to the area in which it manifested, and the largest voltage oscillation magnitudes have been observed near the connection points of three solar farms in the region[4]. Therefore, the impedance analysis has primarily focused on these three solar farms, respectively SF1, SF2, and SF3.

Combining the field measurement analysis and the study methodology, the following study procedure was adopted for this work:

- In the first step, impedance scans were performed separately at the three solar farms connected in a SMIB configuration. The stability of each solar farm was determined using their impedance response for different SCR and X/R ratio of a hypothetical inductive grid at their connection points.
- In the second step, impedance scans were performed at the three solar farms connected in the wide area network model. The stability of the wide area system was determined in this step for different operating and dispatch conditions at the three solar farms, to determine each of their impact to the system stability. The impedance scans considered different permutations of the following potential contributing factors: solar farm active power output, solar farm reactive power output, solar irradiance levels, solar farm dispatch status (wide area network scan only), and network outage conditions (wide area network scan only).

3 Impedance-based analysis with solar farms connected in SMIB configuration

This section of the report presents the impedance-based analysis for each solar farm (SF) connected in SMIB configuration, with different SCR and X/R conditions. This analysis revealed the internal resonance modes of each SF, and under what grid SCR and X/R condition each SF would become unstable.

3.1 Solar farm 1 (SF1)

Figure 2 shows the sequence admittance response of SF1 from the 66 kV connection point bus for high and low irradiance conditions obtained by connecting the farm in a SMIB configuration. In both cases, the solar farm was dispatched with an active power setpoint which could only be achieved with a high irradiance level, therefore when running with a low irradiance, the solar farm would operate at an active power output lower than its setpoint.

It can be seen from **Figure 2(b)** that for the low irradiance condition, SF1 exhibits an underdamped resonance near 17 Hz in $Y_{nn}(s)$ element of the sequence admittance response. It is possible that this underdamped resonance is responsible for the 17 Hz oscillations in the WMZ power system.

Figure 2 Sequence admittance response of SF1 for (a) high irradiance and (b) low irradiance conditions

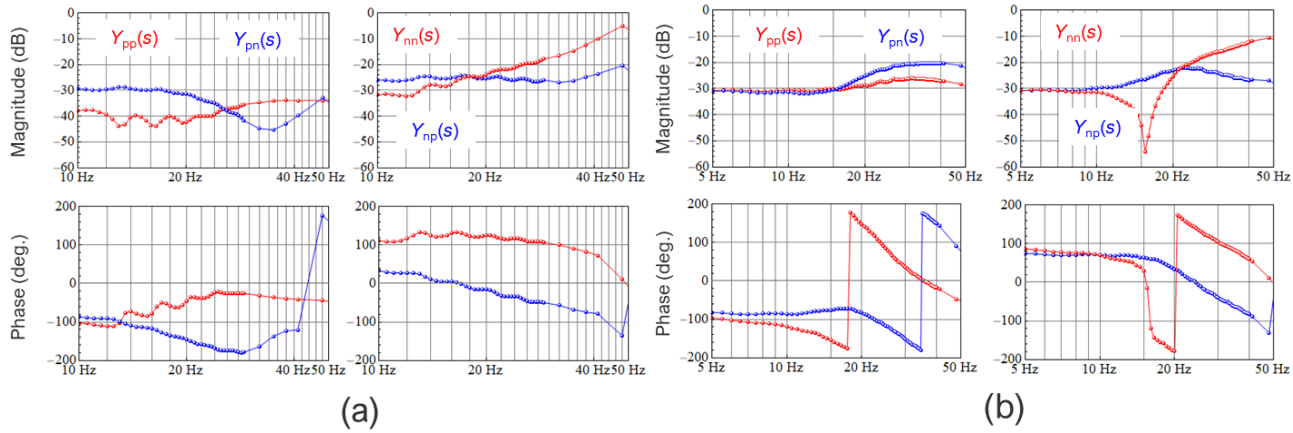

Figure 3 shows the results of the impedance-based stability analysis at SF1 under the low irradiance condition using the impedance response shown in **Figure 2(b)** for two different grid conditions. The modal impedance response of $Z_n(s)$ and the Nyquist plot of loop gain $L(s)$ in **Figure 3(a)** indicate that SF1 would be unstable at around 17 Hz when the grid SCR is 2.1. This is evident from the clockwise encirclement of the critical point by the Nyquist plot with the frequency at encirclement being around 17 Hz.

Figure 3 Stability analysis of SF1 under a low irradiance condition in SMIB configuration for two grid strength conditions – (a) SCR = 2.1, X/R = 3.2; (b) SCR = 4.1, X/R = 3.2

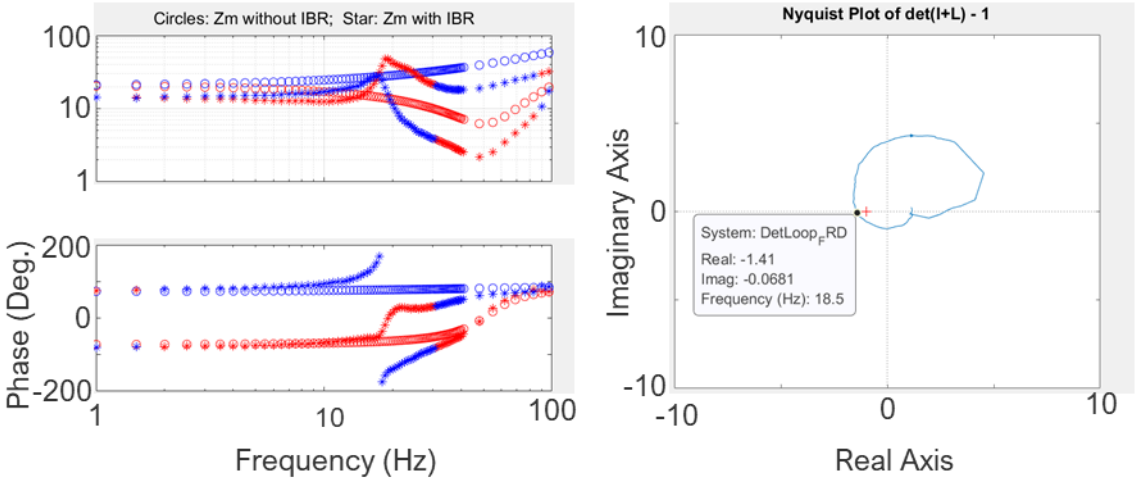

(a)

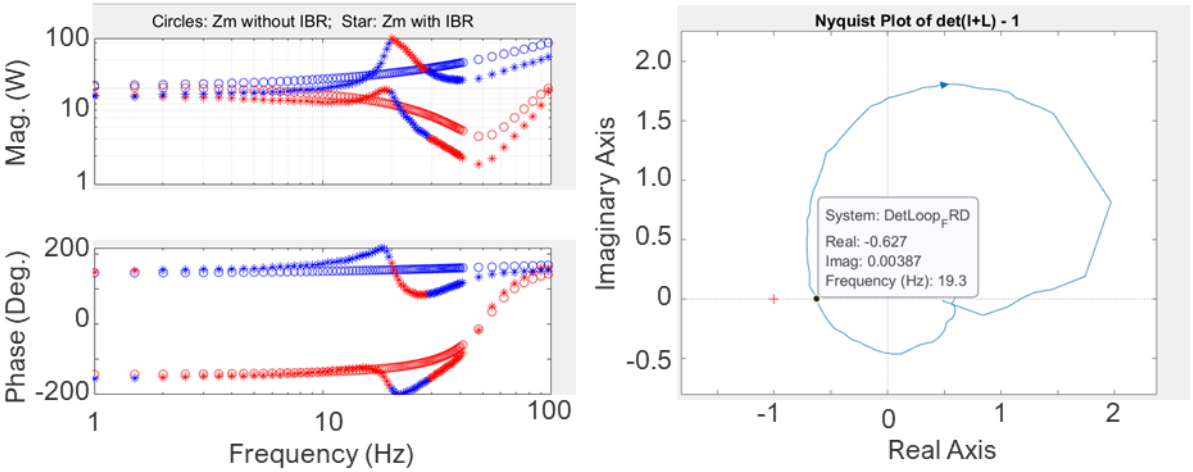

(b)

Figure 3(b) shows stability analysis using the same impedance scan of SF1 from **Figure 2**(b) for grid SCR of 4.1, indicating that the solar farm is stable for a grid SCR of 4.1.

It is important to note that similar analysis can be performed for any grid SCR and X/R ratio in just a few seconds without repeating the impedance scan of the solar farm to identify its stability boundary in terms of the SCR of the grid at the connection point. Time domain simulations (not shown in this report) confirmed the findings from the impedance-based stability analysis.

The above plots are generated directly from the impedance scan and stability analysis tool used for this work. A detailed description of this tool is in Appendix A2 of this report.

3.2 Solar farm 2 (SF2)

Figure 4(a) shows the sequence admittance response of SF2 for a low irradiance condition obtained in the SMIB configuration. It shows an underdamped resonance at 17 Hz similar to SF1 for the low irradiance condition.

Figure 4(b) and (c) shows stability analysis results of the solar farm for the low irradiance condition for grid SCR of 2.1 – they predict instability at around 23.5 Hz. The instability of SF2 near 23.5 Hz was confirmed by time-domain simulations (not shown in this report) of the plant in SMIB configuration. Same as SF1, the instability at SF2 disappears either when the grid at its connection point is stronger with SCR greater than 3 or when the plant irradiance is increased.

Figure 4 Stability analysis at SF2 in SMIB configuration under a low irradiance condition – (a) sequence admittance response of the solar farm, (b) Nyquist plot of loop gain L(s) and (c) modal impedance response of the nodal impedance at the connection point of the solar farm with (plot with asterisks) and without (plot with circles) the solar farm (inductive grid with SCR of 2.1 and X/R ratio of 4 used for the stability analysis)

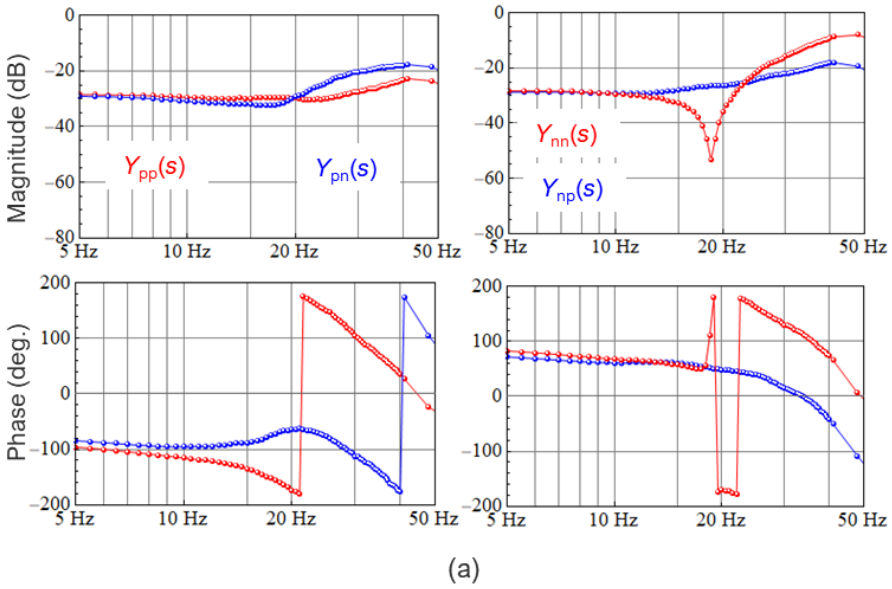

(a)

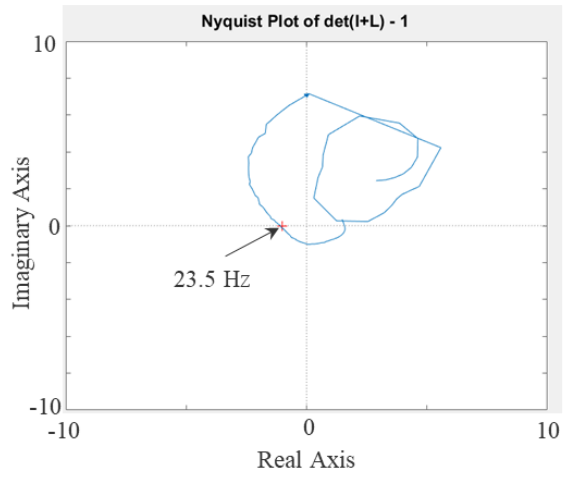

(b)

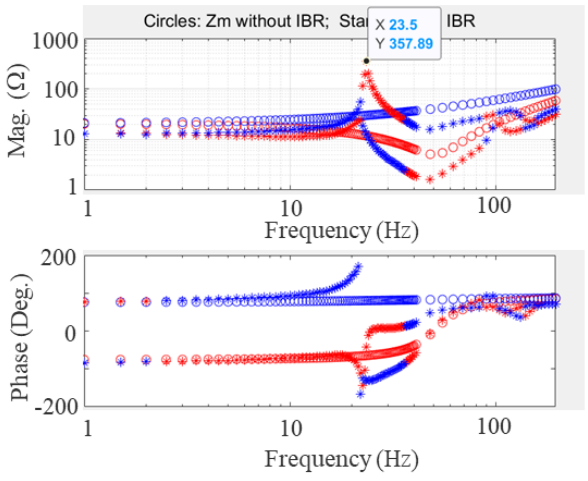

(c)

3.3 Solar farm 3 (SF3)

Figure 5(a) shows the sequence admittance response of SF3 for a low irradiance condition obtained in a SMIB configuration. It shows an underdamped resonance at 17 Hz similar to SF1 and SF2 for the low irradiance condition. **Figure 5(b) and (c)** shows stability analysis results of the solar farm for the low irradiance condition for grid SCR of 2.1 – they predict instability at around 17 Hz, which was confirmed by time-domain simulations of the plant in SMIB configuration. Same as SF1 and SF2, the instability disappears either when the grid is stronger or when the irradiance is increased.

Figure 5 Stability analysis at SF3 in SMIB configuration under a low irradiance condition – (a) sequence admittance response of the solar farm, (b) Nyquist plot of loop gain L(s) and (c) modal impedance response of the nodal impedance at the connection point of the solar farm with (plot with asterisks) and without (plot with circles) the solar farm (inductive grid with SCR of 2.1 and X/R ratio of 3.2 used for the stability analysis)

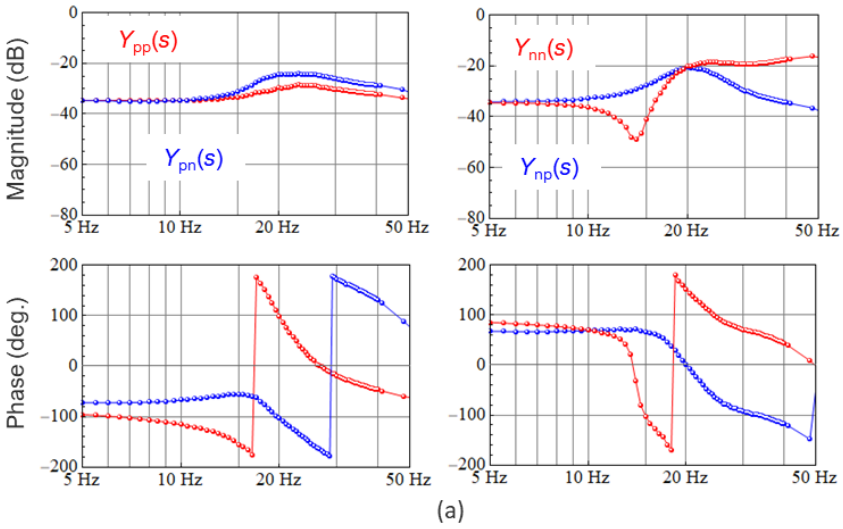

(a)

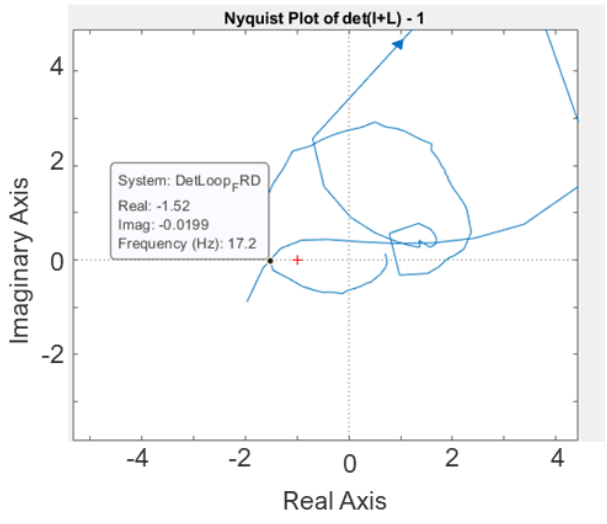

(b)

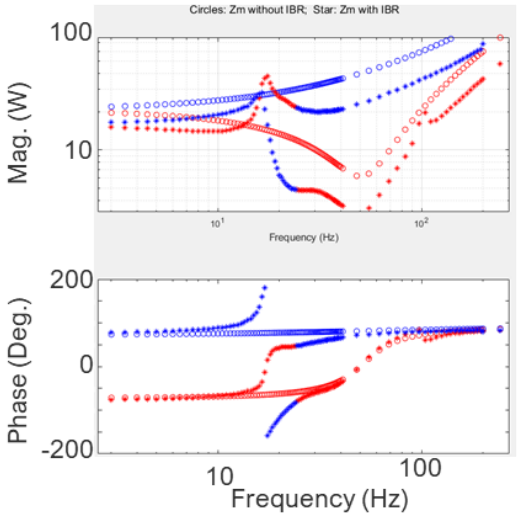

(c)

3.4 Summary

Impedance-based stability analysis at the three solar farms in the SMIB configuration revealed a resonance mode in each of the three farms at 17 Hz for a low irradiance operating condition. It showed that this mode becomes unstable whenever any of the three farms is connected to a weak grid with an SCR at connection point of less than or equal to 2.5.

However, these findings alone do not provide sufficient clarification regarding which of the three farms has the largest contribution to the root cause of the 17 Hz oscillations observed in the WMZ power system.

Moreover, the grid strength at these three solar farms using the positive sequence power flow model of the WMZ system is significantly higher than the grid strength identified by SMIB analysis when the three solar farms become unstable; hence, the weak grid instability found at the three solar farms using the SMIB analysis does not explain the 17 Hz oscillations observed in the WMZ system.

In addition, the impedance-based stability analysis in the SMIB configuration modelled the grid using an ideal voltage source connected in series with an R-L branch. However, the grid impedance seen at the connection point of an IBR can be "modified" by nearby IBRs, so the actual grid impedance seen by the IBR may not be reasonably presented by the impedance of an R-L branch.

The next section will further discuss the impact on the grid impedance of nearby IBRs, and the findings of the impedance-based analysis of the wide area system, when all the solar farms are connected to the wide area power system.

4 Impedance-based analysis with solar farms connected in wide area network

In the wide area network scan study, impedance scans are performed using an EMT model of the entire WMZ system at a selected solar farm to obtain the impedance/admittance response of both the solar farm, and the WMZ grid seen by the solar farm. The analysis prioritised SF3 in the wide area network scan study, because it has the lowest SCR at its connection point among the three solar farms.

First, the grid seen at the connection point of the SF3 is scanned using an operating condition at SF3 that results in stable operation of the wide area system EMT model – this is necessary as the network scan cannot be performed if the wide area system EMT model is unstable. In the next step, the scanned WMZ grid impedance seen from SF3 can be used for impedance-based stability analysis in conjunction with the impedance responses of SF3, obtained either during the wide area network scan or during previous SMIB configuration scans discussed in Section 1.

This process is repeated at other solar farms for different operating and dispatch conditions.

4.1 Wide area impedance-based analysis with SF3

Figure 6 shows the placement of the impedance scan block[8] inserted between SF3 and the rest of the grid in the wide area WMZ network EMT model. The impedance scan tool[9] interfaces with the impedance scan block for measuring the sequence impedance/admittance response of SF3 and the whole WMZ grid as seen from SF3.

[8] This module is compatible with the EMT simulation software, and can be controlled via the impedance scan tool descripted in Appendix A2.

[9] Refer to Appendix A2 for detailed description of the impedance scan tool used for this work.

Figure 6 Placement of impedance scan block to perform impedance scan in the wide area EMT model

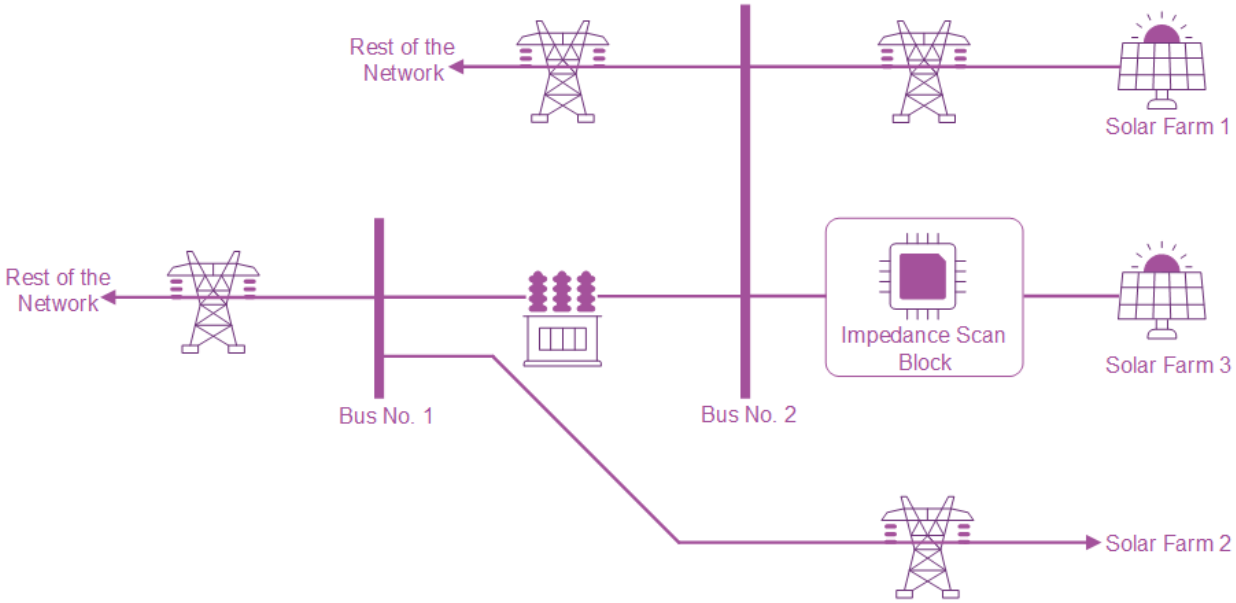

The impedance scan is performed for a few cases using the above wide area EMT model configuration, each with a unique operating condition. The impedance-based stability analysis is then applied to each case focusing on different SFs, starting from SF3, and the findings of the analysis are presented in the following sections.

4.1.1 Base case

The base case considered an operating condition with a low irradiance at SF3 and a high irradiance at SF1 and SF2.

Figure 7(a) shows the sequence admittance response of the WMZ grid seen from the connection point of SF3, obtained from the wide area impedance scan of the base case.

Figure 7(b) shows the Nyquist plot of the loop gain, $L(s)$, using the admittance response of the WMZ grid seen at SF3 (shown in **Figure 7(a)**), and the admittance response of SF3 obtained from previous SMIB analysis during a low irradiance condition as shown in **Figure 5(a)**. Although the Nyquist plot does not encircle the critical point, it is close to an encirclement in the clockwise direction and crosses the real axis at 17 Hz – this indicates that SF3 forms a resonance mode with the grid at around 17 Hz.

The same interpretation can be obtained from **Figure 7(c)**, which shows the response of the modal impedance, $Z_m(s)$, at the connection point of SF3 with the solar farm (plot with asterisks) and without the solar farm (plot with circles). Because the Nyquist plot does not encircle the critical point, it is interpreted that the resonance mode at 17 Hz has positive damping.

The above observations can be verified via EMT time-domain simulation. **Figure 8** shows the time domain response of the three solar farms in the wide area WMZ network EMT model with all IBRs integrated in the model, with a disturbance that reduces the irradiance at SF3. The three solar farms did experience some 17 Hz oscillations, but they are of insignificant magnitude and damped over time, confirming the finding that the 17 Hz mode has positive damping for this operating condition, which is when SF3 has low irradiance but SF1 and SF2 have higher irradiance level.

Figure 7 Stability analysis at SF3 under a low irradiance condition using a wide area network scan obtained when SF1 and SF2 were set up for a high irradiance condition – (a) sequence admittance response of the network seen from SF3, (b) Nyquist plot of loop gain L(s), and (c) modal impedance with (asterisks) and without (circles) SF3 connected to the grid

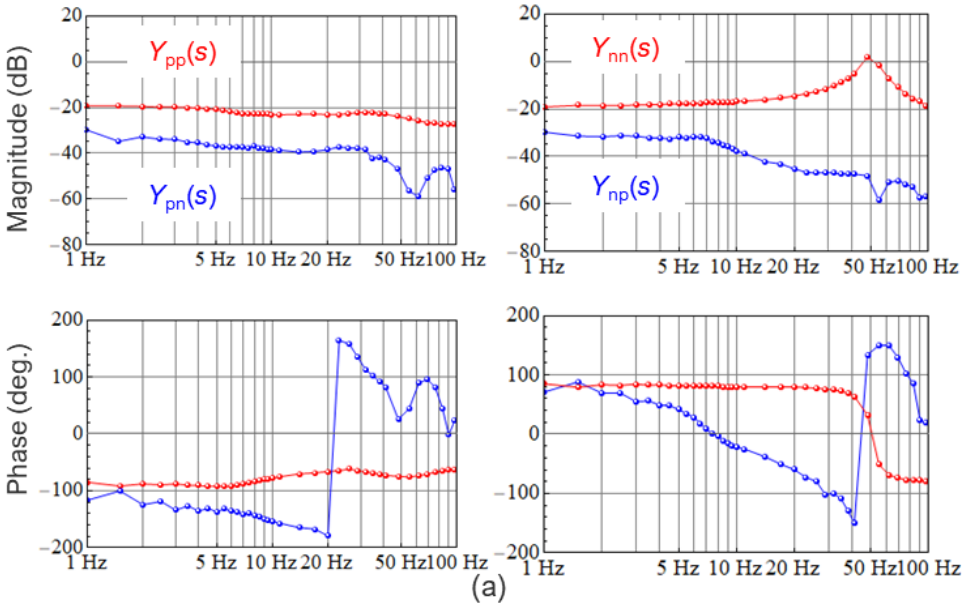

(a)

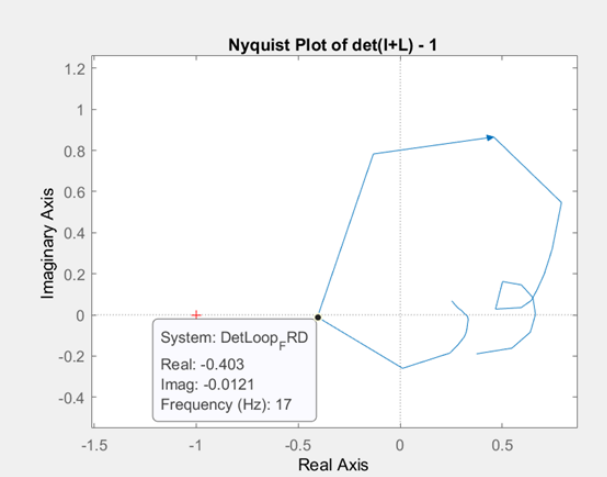

(b)

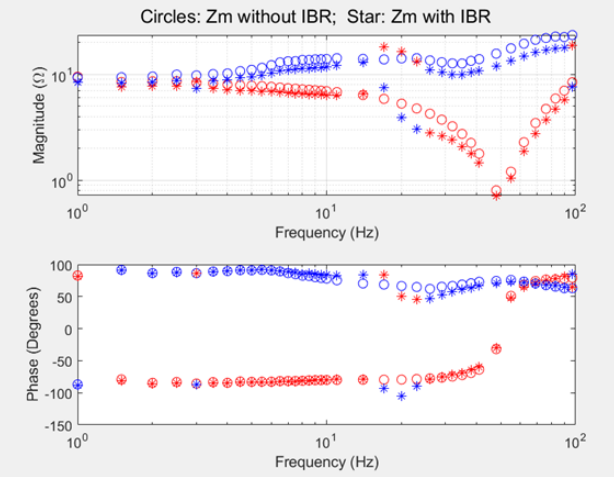

(c)

Figure 8 EMT simulation response of the WMZ system showing stable operation when irradiance at SF3 is changed at t = 16s from a high value (IRR = 600) to a low value (IRR = 180) – the irradiance at SF1 and SF2 was kept unchanged at a high value (IRR = 800) – (left) SF3 time domain P,Q,V response, (middle) SF2 time domain P,Q,V response, (right) SF1 time domain P,Q,V response

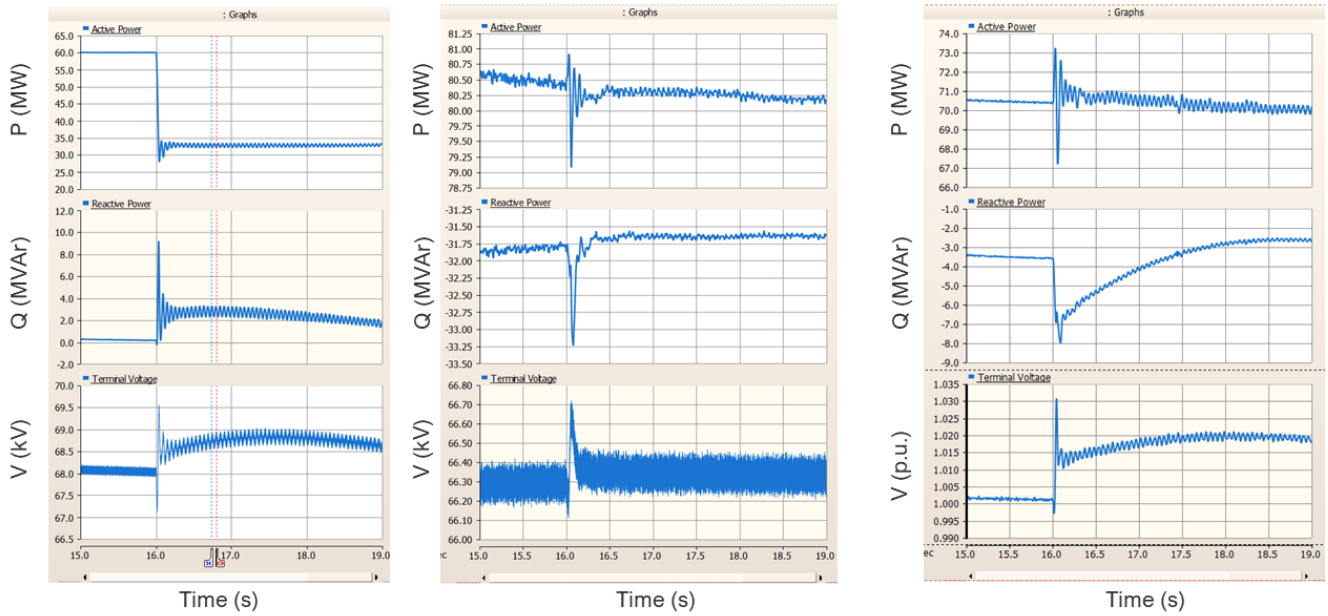

4.1.2 Stressed case

The stressed case considered an operating condition with low irradiance levels at SF1, SF2 and SF3.

As **Figure 9(a)** shows, the grid impedance seen from SF3, obtained from the wide area scan, now contains a resonance mode at 23 Hz during a low irradiance condition at SF1 and SF2.

Figure 9(b) shows the Nyquist plot of the loop gain, *L(s)*, calculated with the admittance response of the WMZ grid seen from SF3 as shown in **Figure 9(a)** and the admittance response of SF3 during a low irradiance condition obtained from previous SMIB analysis (as shown in **Figure 5(a)**). The resulting Nyquist plot marginally encircles the critical point in a clockwise direction with the frequency at encirclement being 17.2 Hz. This indicates instability or negative damping at around 17 Hz.

The modal impedance response in **Figure 9(c)** also shows that the grid has a damped resonance mode at around 23 Hz in the absence of SF3; the response with SF3 (plot with asterisks) shows that the connection of SF3 moves the 23 Hz mode to 17 Hz and reduces its damping to a low negative value.

Figure 9 **Stability analysis at SF3 under a low irradiance condition using a wide area network scan obtained when SF1 and SF2 were set up for a low irradiance condition – (a) sequence admittance response of the WMZ network seen from SF3, (b) Nyquist plot of loop gain L(s), and (c) modal impedance at the connection point of the SF3 with (asterisks) and without (circles) SF3 connected to the grid**

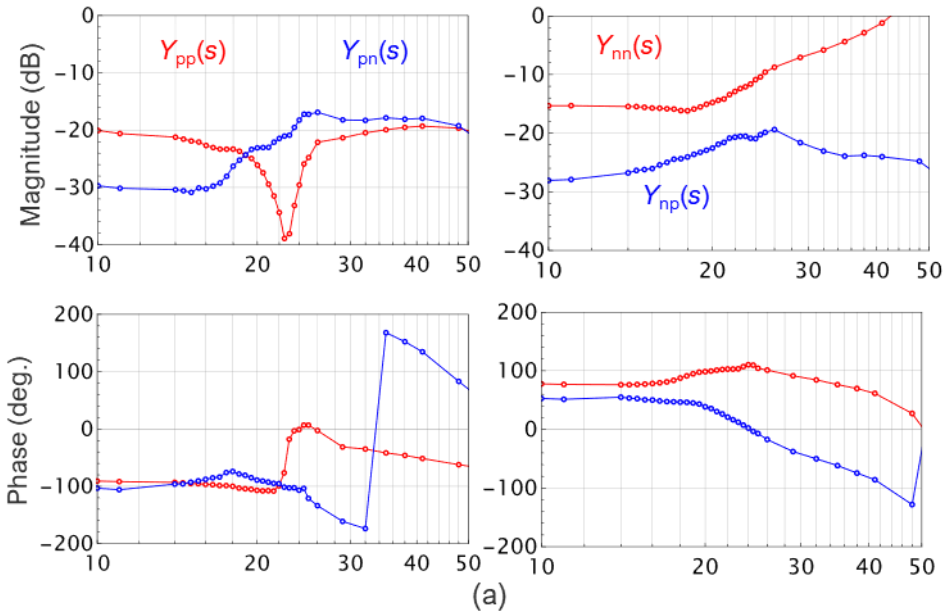

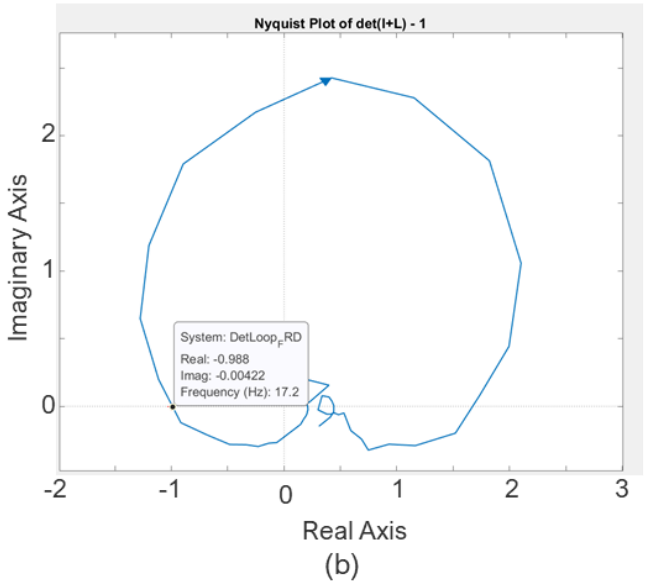

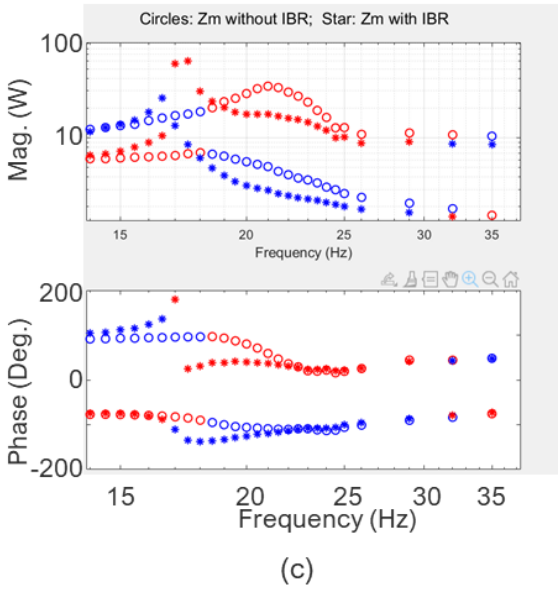

The above analysis shows that SF3 creates an underdamped mode at 17 Hz during a low irradiance condition in the base case of the grid, and the same mode becomes unstable in the stressed case of the grid when SF1 and SF2 also have low irradiance levels. **Figure 10** shows active and reactive power output as well as the voltage at the connection point of the three solar farms for the stressed grid condition, following an irradiance reduction at SF3 (low irradiance level at SF1, SF2). It shows that the system initially operates stably without any oscillations; however, 17 Hz oscillations occur when the irradiance level at SF3 drops to a low level at t = 16s in the simulation.

This confirms the outcome of the impedance-based stability analysis results presented in **Figure 9**, which predicted that for the stressed grid condition (low irradiance level at SF1 and SF2), the reduction in the irradiance level of SF3 will make system unstable at 17 Hz.

Figure 10 EMT simulation response of the wide area system showing unstable oscillations when irradiance at SF3 is changed from a high to a low value –irradiance at SF1 and SF2 was kept unchanged at a low value – (left) SF1 time domain P, Q, V response, (middle) SF3 time domain P, Q, V response, (right) SF2 time domain P, Q, V response

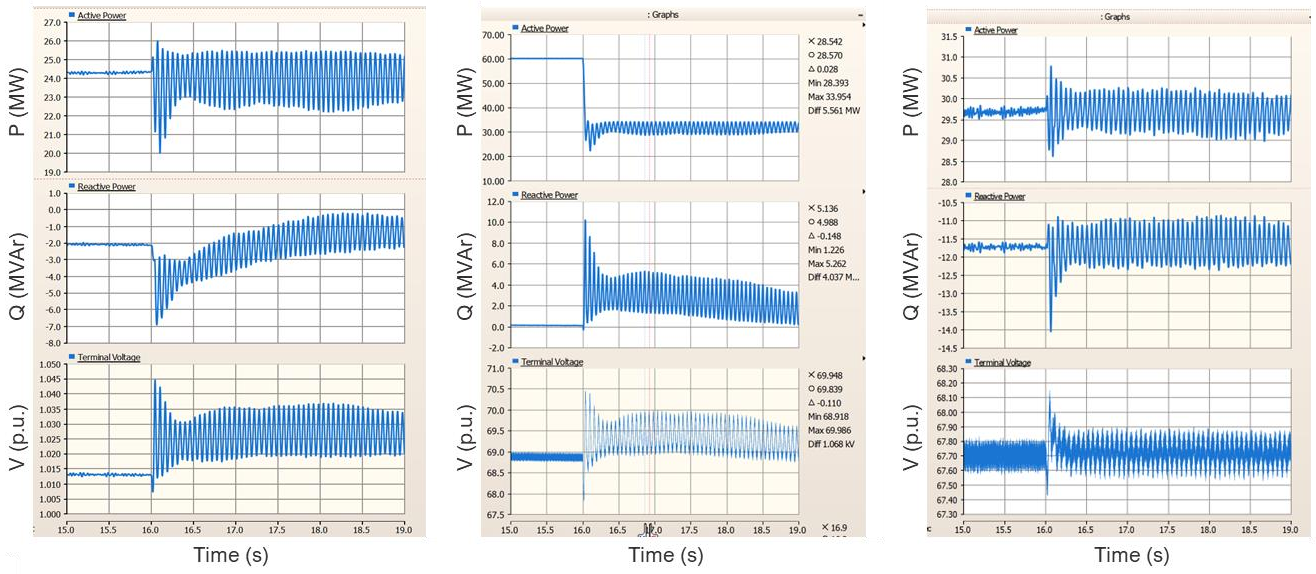

4.1.3 Intermediate cases

The base case and the stressed case represent two bookends in terms of grid conditions seen by SF3. As shown by impedance-based analysis and confirmed by time-domain simulations, SF3 forms an underdamped mode at 17 Hz with the grid for the base case condition, whereas it forms an unstable mode at 17 Hz with the grid for the stressed condition, whenever the irradiance level of SF3 is reduced to a certain level.

Several intermediate cases for the grid condition at the connection point of SF3 were also analysed using impedance scan, in addition to the base case and the stressed case:

- Base Case: SF1 and SF2 have high irradiance levels (IRR = 800).
- Stressed Case: SF1 and SF2 have low irradiance levels (IRR = 180).
- Intermediate Case 1: SF1 and SF2 are offline.
- Intermediate Case 2: SF1 is dispatched at low irradiance level (IRR = 180) and SF2 is offline.
- Intermediate Case 3: SF1 is offline and SF2 is dispatched at low irradiance level (IRR = 180).

The impedance-based stability analysis using wide area network scan for all the five cases described above showed that the 17 Hz mode created by SF3 with the WMZ grid has the highest positive damping for the base case (SF1 and SF2 operate at high irradiance level, IRR = 800) and it has the lowest negative damping for the stressed case (SF1 and SF2 operate at low irradiance level, IRR = 180). Moreover, the damping is very low but positive for the intermediate case 1 when SF1 and SF2 are offline, whereas it is negative for the intermediate cases 2 and 3. This shows that the operation of SF3 at a low

irradiance level is necessary for the existence of instability and oscillations at 17 Hz; the operating/dispatch condition of SF1 and SF2 can improve or reduce the damping of the 17 Hz mode, but they are not the primary contributor to the mode.

This finding from the wide area impedance scan study is confirmed by EMT time-domain simulation results shown in **Figure 11**, which shows that the WMZ system experiences 17 Hz oscillations during the initialization of SF3 at a low irradiance level even when SF1 and SF2 are offline – because of the marginal positive damping in this case, the oscillations eventually damped in steady state. On the other hand, the oscillations continue to persist when SF1 and SF2 are online and operate at a low irradiance level.

Figure 11 EMT simulation response of the WMZ system showing that the operation of SF3 at a low irradiance level is necessary for the existence of instability and oscillations at 17 Hz – the figure shows Q and V response at the connection point of SF3 during simulation initialisation – (left) SF1 and SF2 are dispatched at low irradiance level, (right) SF1 and SF2 are offline

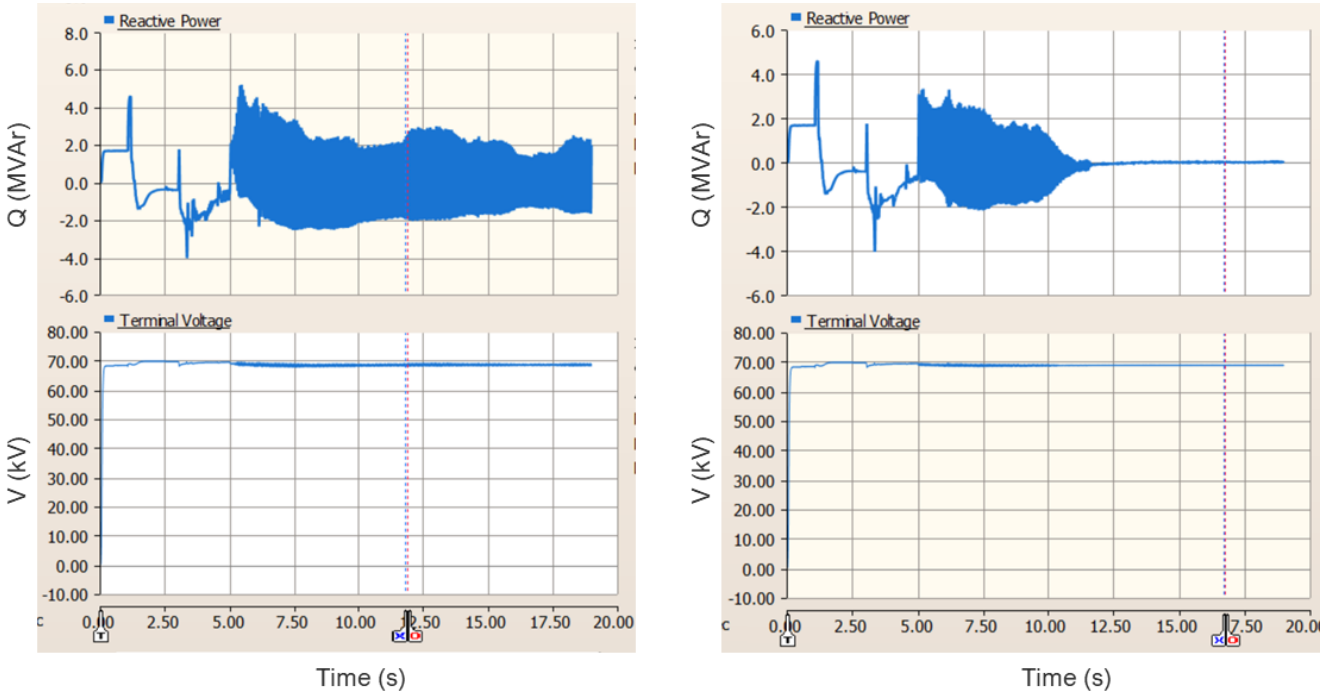

Figure 12 shows the positive-sequence impedance response of the grid seen from SF3 for different scan conditions:

- The black lines show the response when SF1 and SF2 are offline (Intermediate Case 3). It does not show any underdamped resonance in the grid.
- The red lines show the grid impedance response when SF1 and SF2 are dispatched with a high irradiance level. The response is indistinguishable from the black lines, indicating that SF1 and SF2 do not create any new resonance modes in the grid when they have a high irradiance level.
- The blue lines show the grid impedance response when SF1 is dispatched at a low irradiance level and SF2 is offline. It shows an underdamped mode at 73 Hz in the positive-sequence impedance response, which is equivalent to a 23 Hz mode in phasor variables such as power output, voltage magnitude, frequency, etc.

- The pink lines show the response when both SF1 and SF2 are dispatched at a low irradiance level; it shows that the damping of the 73 Hz resonance (again, equivalent to a 23 Hz mode in the phasor domain) is even lower than the previous case.

Figure 12 Positive sequence impedance response of the WMZ grid as seen from SF3 for different dispatch/operating conditions of SF1 and SF2

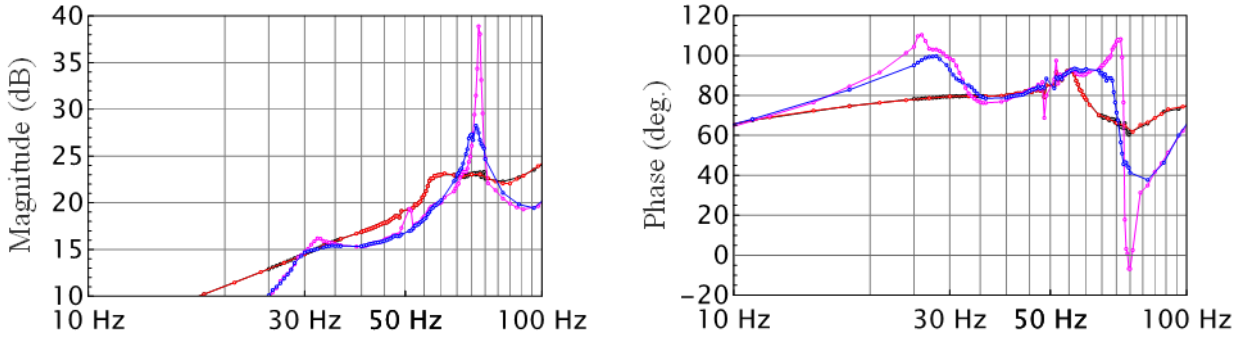

The above findings further emphasise that the grid impedance seen by a specific IBR can be "modified" by the operating conditions of other nearby IBRs, which could alter the outcome of the stability analysis for this specific IBR. It therefore highlights the importance of conducting wide area impedance-based analysis.

4.1.4 Summary

The wide area network scan study presented above at SF3 can be summarised as follows:

- When SF1 and SF2 are online and operate at a low irradiance level, the grid impedance seen at SF3 will contain a 23 Hz resonance mode. This mode is well damped, and will disappear when SF1 and SF2 are operating with high irradiance.
- SF3 creates an underdamped mode at 17 Hz with the WMZ grid even when SF1 and SF2 are offline. The damping of the 17 Hz mode reduces further if either SF1 and/or SF2 are online and operate at a low irradiance level. On the other hand, the damping of the 17 Hz mode improves (increases) when either SF1 and/or SF2 are online and operate at a high irradiance level.
- The wide area impedance scan study also found that the dispatch of SF3 at a low irradiance level is the necessary condition for instability to exist in the WMZ grid at 17 Hz. The dispatch of either SF1 or SF2 at a low irradiance level further deteriorates the stability margin, but removal of either of SF1 or SF2 will not eliminate the possibility of 17 Hz oscillations in the grid.

4.2 Sensitivity analysis of SF1 and SF2 contribution

Once it was confirmed from the wide area network scan study that the dispatch of SF3 at a low irradiance level is the primary source of instability at 17 Hz in the WMZ grid, the focus was moved to studying SF1 and SF2 without dispatching SF3 in the grid to verify the primary contributor to the 23 Hz mode in the grid.

Figure 13 shows one of several results of stability analysis done for conditions when SF3 was not connected to the grid. The figure shows stability analysis at SF1 when both SF1 and SF2 are connected with a low irradiance level. **Figure 13** shows nodal grid impedance response at the connection point of SF1 when SF1 is connected (plot with asterisks) and when SF1 is disconnected (plot with circles). It can be interpreted from the response that SF1 is the primary contributor to the creation

of the 23 Hz mode in the grid, as the 23 Hz mode is absent when SF1 is not connected to the grid. Hence, SF1 is found to be the second significant contributor to oscillations in the WMZ grid after SF3.

Figure 13 Stability analysis at SF1 under a low irradiance condition using a wide area WMZ network scan obtained when SF3 is offline and SF2 is connected at a low irradiance level – (left) modal impedance response at the connection point of SF1 with (asterisks) and without (circles) SF1 connected to the grid, and (right) Nyquist plot of loop gain L(s)

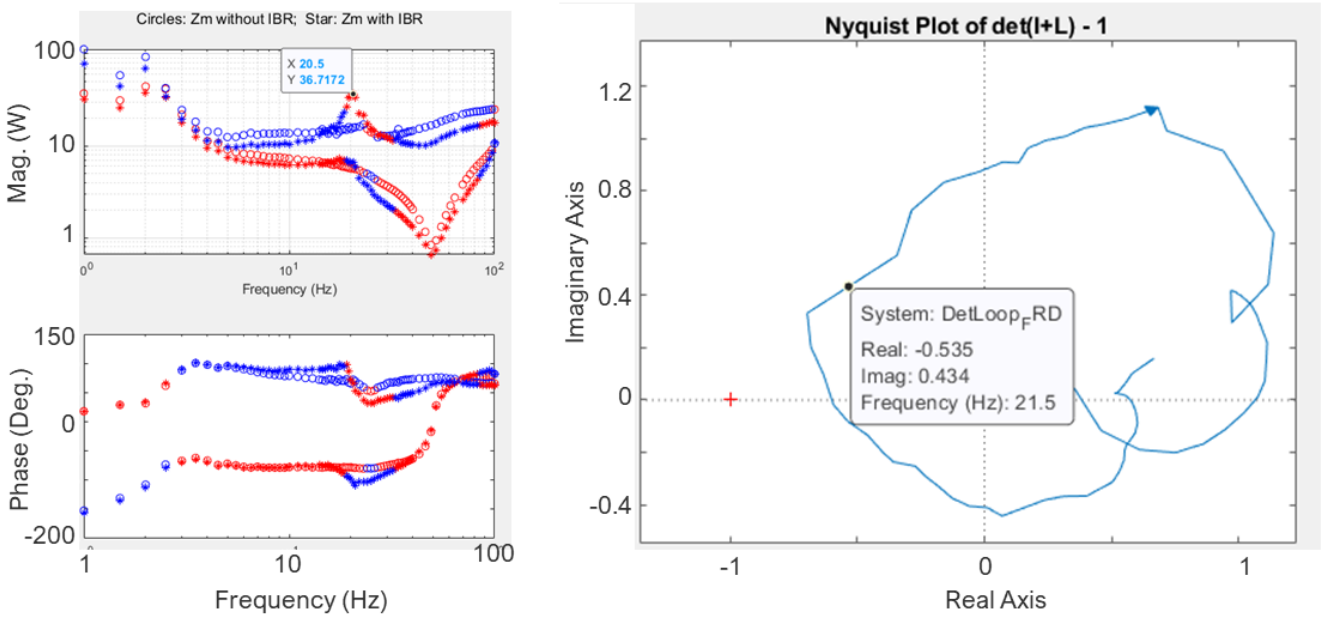

4.3 Impedance-based analysis with revised controls at SF3

The impedance-based analysis has also been applied to assess the effectiveness of control updates which were implemented at SF3, for reducing the risks of 17 Hz oscillations. These control updates were implemented through a collaborative effort among the generator, local NSP, AEMO, and the OEM of the PV inverters at the solar farm.

Figure 14 compares the sequence admittance response of SF3 before and after implementing the control updates. The sequence admittance response is obtained using the same impedance scan tool for a low irradiance condition of SF3 in a SMIB configuration. It can be seen from the sequence admittance response that the 17 Hz mode in the SF3 has disappeared after implementing the control updates, which reduces the risks of 17 Hz oscillations in the WMZ system.

Figure 14 Sequence admittance response of SF3 obtained from 66 kV bus – red, blue lines: response after control updates; black lines: response before control updates

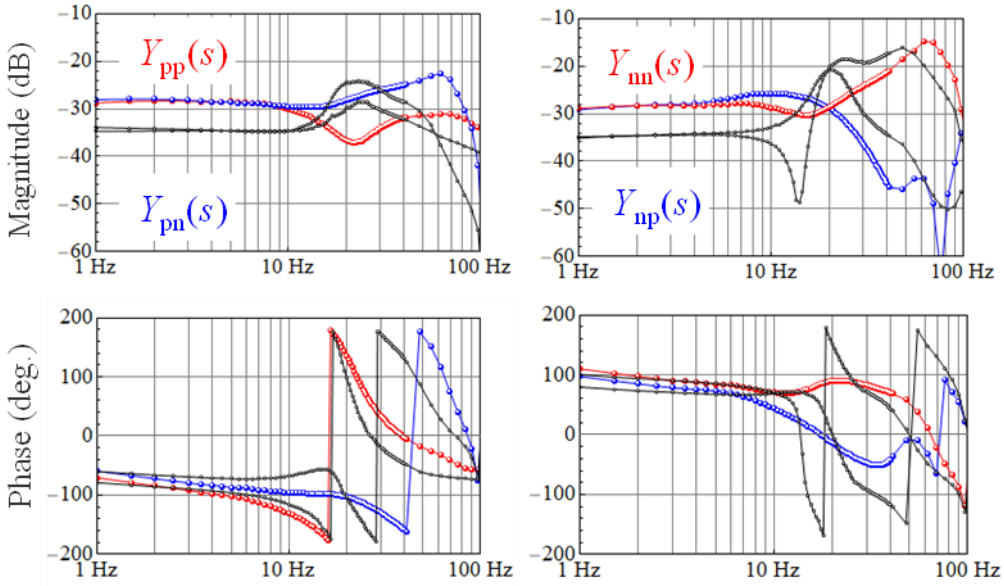

Figure 15 shows the result of the wide area impedance scan-based stability analysis performed at SF3 after implementing the control updates. The stability analysis is performed for stressed condition of the grid at the connection point of SF3; that is, SF1 and SF2 in the WMZ grid are dispatched at a low irradiance level during scanning of the grid impedance from the connection point of SF3.

The modal impedance response at the connection point of SF3 shown in **Figure 15(a)** indicates significant improvement in the damping of the 17 Hz mode after implementing the control updates at SF3 – this is particularly evident when comparing this response with the response shown in **Figure 9(c)** before implementing the control updates.

Comparison of the Nyquist plots in **Figure 15(b)** and **Figure 9(b)** demonstrate the same finding that the damping of the 17 Hz oscillation mode has significantly improved after the control updates.

The response of SF3 shown in **Figure 15(c)** during time-domain simulation initialization of the whole WMZ grid with all three solar farms operating at a low irradiance level confirm the finding that the 17 Hz oscillations are unlikely to occur in the WMZ grid after the implementation of the control updates at SF3.

Figure 15 Stability analysis at SF3 after control updates for a low irradiance condition using a wide area network scan obtained when SF1 and SF2 were also set up for a low irradiance condition – (a) modal impedance at the connection point of SF3 with (asterisks) and without (circles) SF3 connected to the grid; (b) Nyquist plot of loop gain L(s); and (c) EMT simulation response of SF3 during simulation startup at a low irradiance level

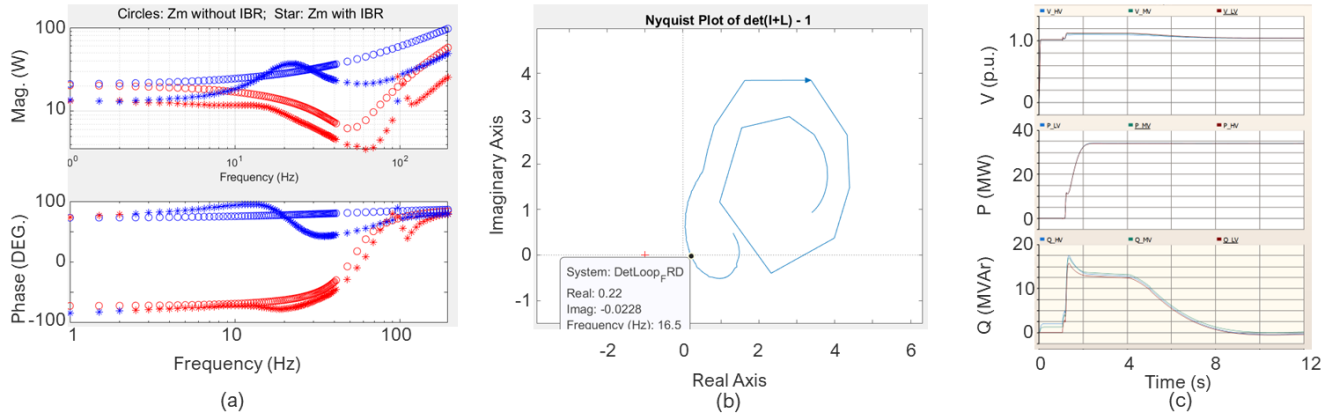

4.4 Summary

The internal 17 Hz modes were first found in all three solar farms during the SMIB analysis. The wide area network scan study showed that under certain dispatch conditions, the 17 Hz modes in the solar farms interact with each other and result in a poorly damped system-wide 17 Hz oscillations. In particular, the dispatch of SF3 at a low irradiance level is found to be the key condition that results in instability and oscillations at 17 Hz in the WMZ system. The operation of SF1 and SF2 at low irradiance levels increases both the stress on the grid and the risk of oscillations at 17 Hz. The contribution to instability of SF1 is found to be higher than that of SF2. Overall, the mitigation strategy for 17 Hz oscillations in the grid should prioritize control updates at SF3 with a focus on eliminating the internal 17 Hz mode in the solar farm.

The results of the wide area impedance assessment are summarised in Table 1.

Table 1 Summary of wide area impedance-based analysis results

Case	Is solar farm connected (Y/N)			Solar farm irradiance level (High/Low)			Resonance mode in grid seen by SF3	Resonance mode in SF3	Overall system resonance mode	Risk of 17 Hz oscillation
	SF1	SF2	SF3	SF1	SF2	SF3				
Base	Yes	Yes	Yes	High	High	Low	None	17 Hz	17 Hz	Low
Stressed	Yes	Yes	Yes	Low	Low	Low	23 Hz	17 Hz	17 Hz	High
Intermediate 1	No	No	Yes	N/A	N/A	Low	None	17 Hz	17 Hz	Medium
Intermediate 2	Yes	No	Yes	Low	N/A	Low	23 Hz	17 Hz	17 Hz	High
Intermediate 3	No	Yes	Yes	N/A	Low	Low	None	17 Hz	17 Hz	Medium
Sensitivity 1	Yes	Yes	No	Low	Low	N/A	23 Hz	17 Hz	None	None
Sensitivity 2	No	Yes	No	N/A	Low	N/A	None	17 Hz	None	None

5 Summary

The impedance scan study of the WMZ in the NEM power system has provided several insights regarding the root causes of 17 Hz oscillations observed in the field. The impedance scan study has shown that such analysis is not only able to identify the largest contributors to oscillations or instabilities in power systems with a high penetration level of IBRs, but can also confirm the mechanism by which each IBR is contributing either positively or negatively to the stable operation of a power system. Impedance-based analysis can support small-signal stability analysis by using vendor-supplied black-box EMT models of IBRs which were already available to the system operator.

The impedance scan study found an internal 17 Hz mode in three solar farms in the wide area WMZ power system; this mode becomes unstable for certain operation/dispatch conditions of the three solar farms, resulting in the 17 Hz oscillations that have been observed in the field.

Specifically, the dispatch of one particular solar farm (SF3) at a low irradiance level was identified as a necessary condition for the 17 Hz oscillations.

It was also found that the dispatch of the other two solar farms (SF1 and SF2) at a low irradiance level can further reduce the damping of the 17 Hz oscillations. However, removal of either of these solar farms will not eliminate the risk of 17 Hz oscillations.

It was found from the wide area impedance-based analysis that certain IBRs can increase the effective grid impedance at non-fundamental frequencies at the connection point of other IBRs. Such an increase in the grid impedance would further reduce the grid strength at non-fundamental frequencies, which can increase the risk of unstable or poorly damped oscillations.

This highlights the limitation of metrics such as the SCR in quantifying grid strength, as such metrics focus only on power system behaviour at the fundamental frequency. Impedance response over a broad frequency range can more effectively estimate grid strength for power systems with a high IBR penetration level.

To date, the revised control system has found to be performing as expected in managing 17 Hz oscillations in the West Murray area. This observation further demonstrates the effectiveness of the impedance-based analysis in investigating sub-synchronous control system oscillations.

A1. Impedance-based stability analysis framework

This appendix provides a detailed description of the impedance-based stability analysis framework utilized for this work. This framework and the associated toolbox are developed by NREL, based on existing publications and practices, including those of NREL. The following content are provided to AEMO by NREL.

Despite AEMO's best effort in verifying the following information, the following content may not include all the details of the impedance-based stability analysis framework developed by NREL. The content below is fully referenced, and readers are encouraged to refer to relevant references and publications for further details.

A1.1 Standard approach

The standard approach for the impedance-based stability analysis uses the impedance response of an IBR, say $Z_i(s)$, and the impedance of the grid at the IBR connection point, say $Z_g(s)$, to evaluate whether the connection of the IBR to the grid will create any resonance mode(s) with insufficient or negative damping[8]. It has been used to analyse many different IBR small signal stability problems[10]. **Figure 16** illustrates how the small-signal dynamics of a grid-connected IBR can be described by a negative feedback loop based on a Norton equivalent of the IBR with internal impedance $Z_i(s)$ and a Thevenin equivalent of the grid with impedance $Z_g(s)$. The loop gain $L(s)$ of the negative feedback loop is given by:

$$L(s) = \frac{Z_g(s)}{Z_i(s)} \quad (1)$$

According to the standard impedance-based stability criterion, the IBR will operate stably if the loop gain, $L(s)$, satisfies the Nyquist criterion. The standard approach for the impedance-based stability analysis method assumes that the grid is stable without the IBR (i.e., when $Z_i(s) = \infty$) and that the IBR is stable if it is connected to an ideal grid with zero internal impedance (i.e., when $Z_g(s) = 0$). If these two assumptions are satisfied, the stability of an IBR – grid system can be determined by checking clockwise encirclements of the critical point (-1, 0) on the complex s-plane using the Nyquist plot of loop gain $L(s)$. If the Nyquist plot of $L(s)$ encircles the critical point in the clockwise direction when the frequency is traversed from a low value to a high value, the IBR will be unstable when connected to the actual grid. The frequency of instability is determined from the frequency at which the Nyquist plot of $L(s)$ encircle the critical point. In the absence of any encirclement of the critical point in the clockwise direction by the Nyquist plot of $L(s)$, which implies that the IBR is stable when connected to the grid, the frequency and damping of any resonance mode formed by the interconnection of the IBR with the grid are determined by frequency at which the Nyquist plot enters the unit circle and the angle at the entry point[11,12].

[10] C. Buchhagen, C. Rauscher, A. Menze, and J. Jung, "BorWin1 – first experiences with harmonic interactions in converter-dominated grids," in Proceedings of 2015 International ETG Congress, Bonn, Germany.

[11] M. Lwin, R. Kazemi, and D. Howard, "Frequency scan considerations for SSCI analysis of wind power plants," in Proceedings of the 2019 IEEE Power and Energy Society General Meeting (PESGM), Atlanta, GA.

[12] J. Shair, X. Xie, W. Liu, X. Li, and H. Li, "Modeling and stability analysis methods for investigating subsynchronous control interactions in large-scale wind power systems," Renewable and Sustainable Energy Review, Vol. 135, pp. 110-420, Jan. 2021.

Figure 16 Impedance-based stability criterion for analysing interaction between an inverter-based resource (IBR) or a power converter and the grid at its connection point – (a) partitioning of a converter-grid system; (b) circuit representation and (c) feedback loop representation of small-signal dynamics

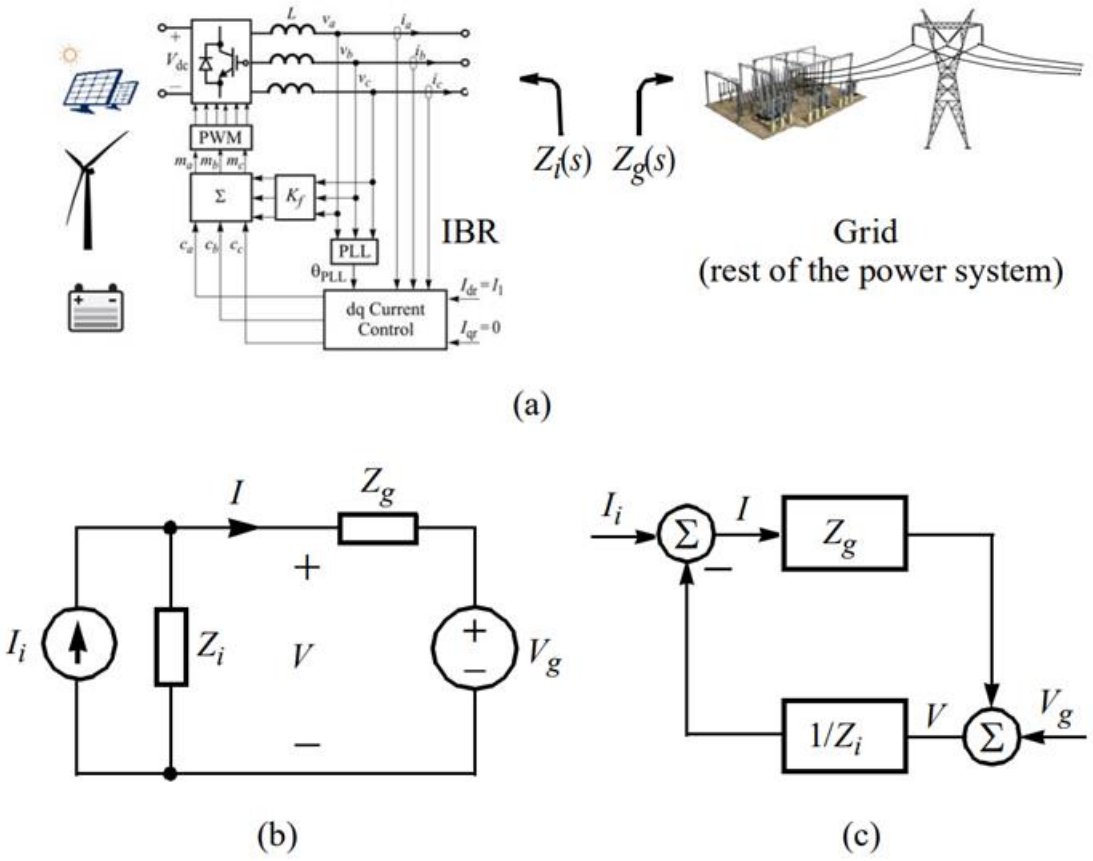

The impedance response of IBRs and the grid exhibits a frequency coupling effect, which couples the positive-sequence and negative-sequence dynamics at certain frequencies, because of which the impedance response of the IBR and the grid must be represented by 2x2 transfer matrices[13,14].

A1.2 Limitations of the standard approach

While the standard form of the impedance-based analysis is effective for a single IBR system, it faces scalability issues when applied to a large power system with multiple IBRs connected. The stability of such a large power system can be analysed using the standard form of the impedance-based stability analysis method by applying the generalized Nyquist criteria to the following loop gain (bold letters indicate higher order matrices to differentiate non-bold letters used in previous section for 2nd order matrices):

$$\boldsymbol{L}(\boldsymbol{s}) = \boldsymbol{Z}_{\boldsymbol{g}}(\boldsymbol{s}) \cdot \boldsymbol{Y}_{\boldsymbol{i}}(\boldsymbol{s}) \tag{2}$$

[13] S. Shah and L. Parsa, "Impedance modeling of three-phase voltage source converters in dq, sequence, and phasor domains," IEEE Transactions Energy Conversion, vol. 32, no. 3, pp. 1139-1150, Sep. 2017.

[14] S. Shah, "Impedance of three-phase systems in dq, sequence, and phasor domains," IEEE Power and Energy Society Publications Webinar Series, Aug. 2020. [Recording Link]: https://resourcecenter.ieee-pes.org/education/webinars/pes_ed_web_dq_0081820_sld.

where $\boldsymbol{Z_g(s)}$ is a transfer matrix representing the impedance of the transmission network looking from the connection points of all the IBRs, and $\boldsymbol{Y_i(s)}$ represents a diagonal transfer matrix with admittances of all the IBRs as its diagonal elements. If there are n IBRs in the network, both $\boldsymbol{Z_g(s)}$ and $\boldsymbol{Y_i(s)}$ are at minimum n^{th} order transfer matrices. Moreover, if frequency coupling between the positive- and negative-sequence dynamics is considered[14], which is generally quite significant at frequencies below 100 Hz and cannot be ignored for the analysis of oscillations at low frequencies below 100 Hz, the order of $\boldsymbol{Z_g(s)}$ and $\boldsymbol{Y_i(s)}$ would be 2n. Hence, significant effort would be required to obtain the impedances of (i) all IBRs involved in the system, including those which are of no interest to system operators, and (ii) that of the network looking from the connection points of all IBRs in the system[15]. The standard approach does not provide flexibility to focus on only a few specific IBRs during stability analysis.

In addition to the above limitation of the standard approach, it is extremely difficult to obtain the network impedance matrix $\boldsymbol{Z_g(s)}$ for a large, real-world power system. Measurement of $\boldsymbol{Z_g(s)}$ requires numerous perturbation experiments involving the injection of perturbation from different connection points of IBRs and measurement of responses at all the connection points, which is time-consuming. IBRs must be isolated from the network model and replaced as current sources during the scanning process. Because the network might contain more complex equipment such as STATCOMs or synchronous condensers, the network-breaking method is not feasible for large real world power systems. Moreover, the voltage and current measurements obtained during different perturbation experiments must be synchronised with the same reference, which further makes the data processing for frequency scanning of the network very challenging. Therefore, frequency scans for obtaining the network impedance matrix $\boldsymbol{Z_g(s)}$ are cumbersome and impractical for a large, real-world power system for which running even a few seconds of EMT simulations can take a significant amount of time.

A1.3 Reversed approach

A reversed approach has been developed to circumvent the above limitations of the standard approach for the impedance-based stability analysis of large power systems with numerous IBRs[16]. The reversed approach focuses on determining how one selected IBR contributes to the stability or instability of the power system, including contribution to control system interaction with other facilities. Because the reversed approach looks at only one IBR at a time, it requires the impedance/admittance response of only the selected IBR and the rest of the network (including other IBRs) as seen from the connection point of the selected IBR. This process can be repeated at any number of IBRs to evaluate how each of them impact the stability of the power system, therefore it greatly simplifies the impedance scan process for a large power system. In addition, the reversed approach allows one to scan the impedance of a device (IBR) and network at its connection point without breaking the network, by enabling network scan directly in the integrated EMT model from the IBR connection points.

The reversed approach can be summarized as follows: if a power system is stable when an IBR is connected to it, then the stability of the power system when the IBR is disconnected can be determined by checking for counterclockwise encirclements of the critical point by the Nyquist plot of loop gain $L(s)$. The power system remains stable when the IBR is disconnected if the Nyquist plot does not encircle the critical point, and the power system will become unstable if the Nyquist plot encircles the critical point in the counterclockwise direction. Moreover, the change in frequency and damping of a resonance mode of a power system when an IBR is disconnected can be determined from the nodal impedance

[15] S. Shah, W. Yan, P. Koralewicz, E. Mendiola, and V. Gevorgian, "A reversed impedance-based stability criterion for IBR grids," in Proc. 21st Wind and Solar Integration Workshop, The Hague, Netherlands, Oct. 2022. [Online]: https://www.nrel.gov/docs/fy23osti/84000.pdf.

response at the connection point of the IBR under both connected and disconnected status of the IBR. The nodal impedance at the connection point of an IBR, such as the one shown in **Figure 2(a)**, is defined as follows:

$$Z_n(s) = \begin{cases} Z_g(s) & \text{without IBR} \\ \frac{Z_g(s) \cdot Z_i(s)}{Z_g(s) + Z_i(s)} & \text{with IBR} \end{cases} \quad (3)$$

Note that the loop gain $L(s)$ and impedances $Z_g(s)$, $Z_i(s)$, and $Z_n(s)$ are all second-order transfer matrices (2 x 2 matrix) when frequency coupling between the positive- and negative-sequence dynamics is considered, which is critical for the analysis of sub-synchronous oscillations. The eigen values of the nodal impedance $Z_n(s)$ at each frequency point is called the modal impedance response and it is denoted as $Z_m(s)$.

A1.4 Validity of the reversed approach

Unlike the standard approach where the grid is assumed to be stable without an IBR and one evaluates if the integrated IBR-grid system will remain stable when the IBR is connected, the reversed approach starts with the assumption that the integrated IBR-grid system is stable, and one evaluates if the grid will remain stable or not when the IBR is disconnected. Because the starting point in the reversed approach is that the integrated IBR-grid system is stable, the impedance/admittance scans of the IBR and the grid at its connection point can be performed directly on the integrated IBR-grid EMT model without breaking the model into two pieces containing the IBR and the grid respectively. However, one common question that is raised whenever the reversed approach is explained for the first time is how one can assume that the power system is stable with all the IBRs when one is trying to find the root cause of instability or oscillations? This question is answered in the following paragraph.

When an instability or oscillations are observed in a region with IBRs, to apply the standard approach of the impedance-based stability analysis, one must divide the system into two parts: the first part being the grid that is known to be stable in the absence of certain (or all) IBRs, and the second part being the IBRs that are removed from the system to create the first part. In this approach, we are asking the question if the connection of the selected IBRs to the grid will become unstable or not. As explained previously, this standard approach is not scalable, and it is very difficult to apply to a large, real power system. Any power system that experiences an instability or oscillations can be assumed to be stable before the instability or oscillations are observed, either due to a change in system topology or operating conditions. The reversed approach aims to analyse the system that was stable before the appearance of an instability to evaluate how selected IBRs are contributing to the stability or instability of the power system. When a change in the system topology or operating condition creates an instability, it is reasonable to assume that the contribution of an IBR to instability or stability of the system would not change significantly from the previous stable state under which the impedance-based stability analysis is performed.

A detailed description of the reversed approach can be found in NREL's publication[16].

A2. Grid Impedance Scan Tool (GIST)

The impedance-based stability analysis process followed in this work focuses on one IBR at a time for evaluating its impact on the stability of the WMZ power system. The process is repeated sequentially at other IBRs to evaluate each of their impact to the grid stability. This approach requires the impedance response of the IBR being analysed, and the grid impedance seen at the connection point of the IBR which also includes other IBRs in the system, measured using the software Grid Impedance Scan Tool (GIST) developed by NREL[16,17].

Figure 17 shows the graphical user interfaces and the impedance scan block of the GIST software. In practice, the impedance scan block is inserted between an IBR and the rest of the grid in a compatible EMT simulation environment. This block successively injects voltage perturbations of different frequencies in series between the IBR and the rest of the grid and records the three-phase voltages and currents on both sides for further processing. The frequency range, resolution, magnitudes of the perturbation voltage signal, and length of measurement windows are adjustable by the GIST software as specified by the user before initiating the scan process. These scan parameters can be specified to be different for different frequency range, for example, the length of the measurement window can be specified to be larger for lower perturbation frequencies compared to that for higher perturbation frequencies. The recorded data are then post-processed to derive and plot impedance/admittance responses of the IBR and the grid. The stability analysis at IBR can then be conducted using the scanned IBR impedance response in conjunction with either the scanned impedance response of the grid (wide area network analysis), or a grid strength condition specified in terms of SCR and X/R ratio (SMIB analysis).

Figure 17 NREL's Grid Impedance Scan Tool (GIST) user interface and EMT module

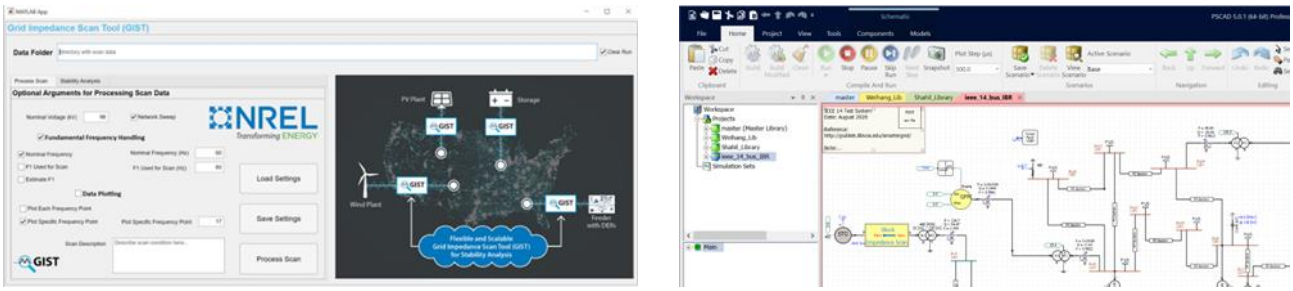

The impedance measurement process is automated, and the measured impedance can be reused for the stability analysis with the impedance measurement from the SMIB scans. The impedance measurement for an IBR in a SMIB configuration took around 2-4 hours for one operating condition, depending on the frequency range and resolution, while it took around 2-4 days to complete an impedance measurement in a wide area network model for one operating condition. There are several reasons for exceedingly long scan time:

- The size and complexity of the wide area network model including all the IBR models implied that EMT simulations run at much slower speeds compared to EMT simulations of a single IBR in SMIB configuration.

[16] S. Shah, P. Koralewicz, and E. Mendiola, GIST (Grid Impedance Scan Tool) [SWR-22-73]. Computer software. USDOE Office of Energy Efficiency and Renewable Energy (EERE), Renewable Power Office. Wind Energy Technologies Office. 21 Sep. 2022. Web. doi:10.11578/dc.20221214.3.

[17] "Impedance Measurement." NREL.gov. https://www.nrel.gov/grid/impedance-measurement.html.

- The wide area model needs to run till steady state for each frequency point in the frequency scan before voltage perturbations are injected for obtaining the network impedance. This is because many of the IBR Blackbox models in the WMZ network model did not support the snapshot feature of EMT which allows starting the simulation of a model from a pre-defined time when the system has already reached a steady state.

A snapshot feature would eliminate the need for running the initial part of the EMT simulation for each perturbation frequency until steady state operation is reached, which is around 15 seconds of EMT simulation run; this can significantly reduce the scan time of the network from 2-4 days to around 8-12 hours.

There are other approaches to reduce the impedance scan time of a large network, such as parallelising scan at multiple perturbation frequencies by using a cluster of workstations. The development of the GIST is currently working on such methods to reduce the scan time of large networks such as WMZ to less than a couple of hours.